Ericson, Julia; Palva, Satu; Palva, Matias; Klingberg, Torkel

Strengthening of alpha synchronization is a neural correlate of cognitive transfer

Published in:
Cerebral Cortex

DOI:
10.1093/cercor/bhad527

Published: 01/02/2024

Document Version
Publisher's PDF, also known as Version of record

Please cite the original version:
Ericson, J., Palva, S., Palva, M., & Klingberg, T. (2024). Strengthening of alpha synchronization is a neural correlate of cognitive transfer. *Cerebral Cortex*, *34*(2), Article bhad527. https://doi.org/10.1093/cercor/bhad527

Cerebral Cortex, 2024, **34**, 1–11

https://doi.org/10.1093/cercor/bhad527

Advance access publication date 13 January 2024

Original Article

Strengthening of alpha synchronization is a neural correlate of cognitive transfer

Julia Ericson[1], Satu Palva[2,3], Matias Palva[2,3,4], Torkel Klingberg[1,*]

[1]Department of Neuroscience, Karolinska Institutet, 17177 Stockholm, Sweden,
[2]Neuroscience Center, HiLIFE-Helsinki Institute of Lifescience, University of Helsinki, 00014 Helsinki, Finland,
[3]Centre for Cognitive Neuroimaging (CCNi), School Psychology and Neuroscience, University of Glasgow, Glasgow G12 8QQ, Scotland,
[4]Department of Neuroscience and Bioengineering (NBE), Aalto University, 00076 Aalto, Finland

[*]Corresponding author: Department of Neuroscience, Karolinska Institutet, 17177 Stockholm, Sweden. Email: torkel.klingberg@ki.se

Cognitive training can lead to improvements in both task-specific strategies and general capacities, such as visuo-spatial working memory (VSWM). The latter emerge slowly and linearly throughout training, in contrast to strategy where changes typically occur within the first days of training. Changes in strategy and capacity have not been separated in prior neuroimaging studies. Here, we used a within-participants design with dense temporal sampling to capture the time dynamics of neural mechanisms associated with change in capacity. In four participants, neural activity was recorded with magnetoencephalography on seven occasions over two months of visuo-spatial working memory training. During scanning, the participants performed a trained visuo-spatial working memory task, a transfer task, and a control task. First, we extracted an individual visuo-spatial working memory-load-dependent synchronization network for each participant. Next, we identified linear changes over time in the network, congruent with the temporal dynamics of capacity change. Three out of four participants showed a gradual strengthening of alpha synchronization. Strengthening of the same connections was also found in the transfer task but not in the control task. This suggests that cognitive transfer occurs through slow, gradual strengthening of alpha synchronization between cortical regions that are vital for both the trained task and the transfer task.

Key words: working memory; cortical plasticity; cortical oscillations; MEG.

Introduction

Behavioral studies show that cognitive training can transfer to other cognitive tasks (Klingberg et al. 2005; Gathercole et al. 2008; Jaeggi et al. 2008; Schmiedek et al. 2010; Judd and Klingberg 2021), but that the training gains can also be tasks specific (Gathercole et al. 2019). Task specific changes could be implicit strategies such as automatization of stimulus–response rules (Shiffrin and Schneider 1977), or explicit strategies only relevant for the trained task and tasks which are very similar (Ericsson et al. 1980). Transferable improvements, on the other hand, refer to enhancement of a more general capacity such as visuo-spatial working memory (VSWM) capacity, spatial ability, inhibitory ability, or IQ (Katz et al. 2018; Smid et al. 2020).

When studying the neural mechanisms of capacity improvement, it is important to disentangle them from strategy related changes. In a previous behavioral study (Ericson and Klingberg 2023), we found that the temporal dynamics of capacity improvement differed from that of strategy. Capacity increased slowly and linearly over several weeks, while strategy development was quick and terminated on average after 3 days of training.

Neuroimaging studies of the neural correlates of VSWM capacity have highlighted the importance of frontoparietal activity, which has been shown using both fMRI and M/EEG (Constantinidis and Klingberg 2016). In particular, neural oscillations in and between these regions are considered fundamental for VSWM (Sauseng et al. 2019). Both local oscillations in frontoparietal regions (Palva et al. 2011; Roux and Uhlhaas 2014) as well as the inter-areal synchronization within (Palva et al. 2010; Chen et al. 2023) and across frequencies have been shown to reflect individual VSWM capacity (Siebenhühner et al. 2016; Berger et al. 2019).

In terms of neural changes induced by VSWM *training*, frontoparietal connectivity appears to be specifically important. During VSWM training, increased functional coupling between frontoparietal regions has been detected with fMRI (Jolles et al. 2013). In M/EEG, training is associated with strengthened frontoparietal synchronization (Kundu et al. 2013) and parieto-occipital synchronicity (Astle et al. 2015). However, these studies compared neural activity before and after training. Repeated measures throughout the training period would give further insight into the temporal dynamics, which is important for differentiating between strategy and capacity.

Repeated measurements limit the number of subjects for practical reasons. In a study with few subjects but many measurements, within-participant statistics is more suitable (Molenaar 2004; Smith and Little 2018; Ince et al. 2022). In the case of cognitive training, within-participant statistics could also be advantageous for two other reasons. First, the architecture of networks employed during complex cognitive tasks can vary substantially between individuals (Thiebaut de Schotten and Forkel 2022). Second, individual behavioral responses to cognitive training differ to the group-averaged response (Ericson and Klingberg 2023),

Received: September 4, 2023. **Revised:** December 15, 2023. **Accepted:** December 16, 2023

which implies that the group averaged neural dynamics might not generalize well either (Fisher et al. 2018).

In this study, we followed four participants over 8 weeks of VSWM training. We scanned the participants on seven occasions during the training period using MEG. To better differentiate between task specific and transferable improvements, the scanning sessions were scheduled to be more frequent in the beginning of the training when most of the improvement on the trained task takes place. More specifically, the subjects were scanned on days 1, 2, 4, 9, 19, 29, and 39. In the scanner, the subjects performed a trained task from the VSWM training program, one non-trained VSWM transfer task and a recognition task that was used as a control. Transfer from the training program to the non-trained VSWM task has previously been established in behavioral studies with several hundred subjects (Bergman-Nutley and Klingberg 2014; Ericson and Klingberg 2023).

We hypothesized that transferable improvement is linked to a strengthened synchronization within VSWM-load-dependent networks, defined individually for each participant. We furthermore hypothesized that these individualized VSWM- load-dependent networks, albeit unique to each participant, would encompass frontoparietal regions. Finally, we hypothesized that the synchronization increase would be linear throughout the training period, reflecting the capacity component described in our previous behavioral study (Ericson and Klingberg 2023).

Although the main aim of the study was to investigate neural correlates of transferable improvement, we also investigated potential neural correlates of strategy. We did not have a prior hypothesis about where strategy-related changes would emerge; however, we expected these changes to occur within the first days of training.

Materials and methods

Participants

The study included five participants aged 20, 21, 21, 22, and 26 (two men). One participant (woman, 20 years) dropped out after the first session and was therefore not included in the analysis. All participants consented to the study and the study design was approved by the Swedish Ethics Committee.

Cognitive training program

The participants trained their VSWM at home using the VSWM training software Cogmed (https://www.cogmed.com), which is comprised of 12 related VSWM tasks. The training sessions were 25 minutes long and spanned over 8 weeks. The participants practiced the VSWM training program on all weekdays, except for the days when scanning was scheduled. Including both training at home and sessions in the scanner, there were 39 training days in total (Fig. 1A). The training was automatically recorded and monitored remotely. All participants completed the full training program of 40 days.

Behavioral improvement

To analyze the behavioral improvement from the training program, we fitted the performance data to a piecewise linear function using a Hidden Markov Model (HMM). According to our behavioral study (Ericson and Klingberg 2023), the HMM can approximate two processes of VSWM training—task-specific strategy development and capacity improvement that transfers to other tasks. During the first phase, both processes are present, while only capacity improvement occurs in the second phase. Thus, if a capacity improvement has occurred during the training, the linear increase should be significant also in the second training phase.

MEG scanning sessions

On days 1, 2, 4, 9, 19, 29, and 39, the participants were scanned using MEG (S1–S7). Each scanning session contained a series of blocks with 20 trials in each block. A block only contained trials of the same sort and of the same level. Between each block, there was a compulsory break of at least 30 seconds. The total length of a session was about an hour. The stimuli were created in Presentation (https://www.neurobs.com/index_html). There were three scanning tasks in total—a trained task, a control task, and a transfer task.

The trained task

The first task (Grid) was a trained task from the VSWM training program, and it was included in all scanning sessions (Fig. 1B). It required the participants to remember a sequence of positions on a 4 × 4 grid, where the level corresponded to the number of cues in the sequence. During training at home, the participants reported the answers by clicking on the grid positions using the computer mouse. However, in the scanner we did not have access to a computer mouse. Instead, a number between 1 and 16 was displayed in each grid position after the trial presentation and the participants reported the numbers that corresponded to the right grid positions verbally. The numbers were shuffled between each trial. A measurement session contained 40 trials of Grid on level 5 and 40 trials on level 6.

The control task

In all scanning sessions, the participants also performed a control task (Fig. 1B). This was a recognition task where a sequence of letters was presented verbally, and the participants had to report whether the letter Q had been presented in the sequence or not. The sequences contained either five or six letters and similarly to the trained task; each session had 40 trials on level 5 and 40 trials on level 6.

The transfer task

Finally, the participant did a transfer task (Fig. 1B) in all sessions except for S3. The transfer task was not part of the VSWM training program, but it was also a working memory task. Here, the participants were shown a sequence of cues, where each cue contained three shapes. Two shapes were identical, while the third differed. The task was to remember the positions of the odd shapes in the sequence. Forty trials on level 5 were included in each session. We excluded the transfer task from S3 in order for the schedule to resemble that of our previous behavioral study (Ericson and Klingberg 2023). In the paradigm used in our behavioral study, with transfer tasks on days 1, 2, 10, 20, 30, and 40, we found no significant task specific strategy development in the transfer task after day 2. Thus, we applied a similar schedule here to minimize the possibility of transfer effects. For this reason, we also limited the number of trials per session to 40.

MEG acquisition and preprocessing

The MEG data were acquired with a 306-channel whole-head MEG system (Elekta Neuromag TRIUX) at a sample frequency of 1000 Hz. Temporal extension of signal space separation (tSSS) method using MaxFilter software was applied to the data to reduce external artifacts, interpolate bad channels, and co-localize recordings in signal space individually for each participant. We then applied independent component analysis

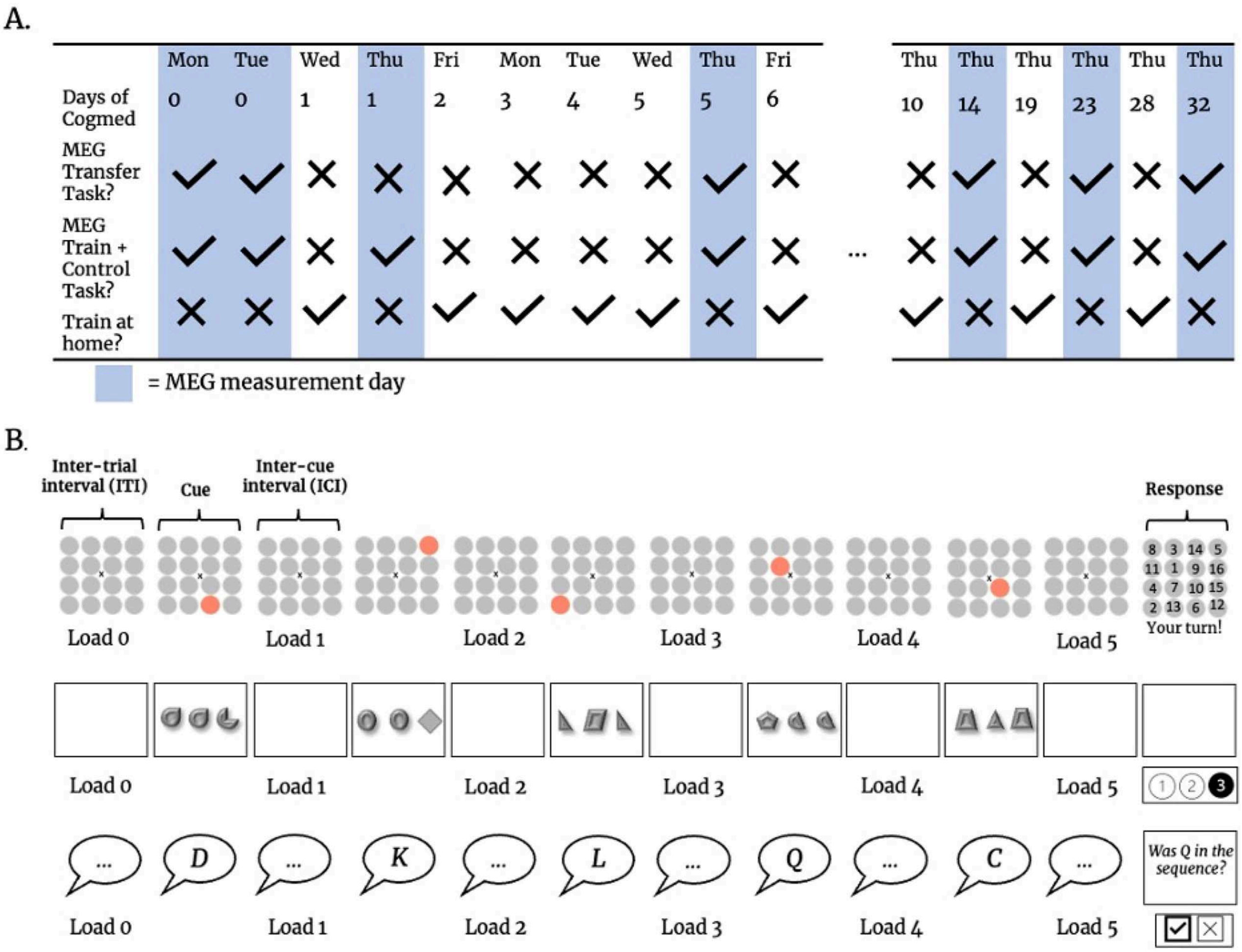

A.

	Mon	Tue	Wed	Thu	Fri	Mon	Tue	Wed	Thu	Fri		Thu	Thu	Thu	Thu	Thu	Thu
Days of Cogmed	0	0	1	1	2	3	4	5	5	6		10	14	19	23	28	32
MEG Transfer Task?	✓	✓	✗	✗	✗	✗	✗	✗	✓	✗		✗	✓	✗	✓	✗	✓
MEG Train + Control Task?	✓	✓	✗	✓	✗	✗	✗	✗	✓	✗	…	✗	✓	✗	✓	✗	✓
Train at home?	✗	✗	✓	✗	✓	✓	✓	✓	✗	✓		✓	✗	✓	✗	✓	✗

Fig. 1. The experimental design. (A) The schedule for MEG-scans and for training. On days 1, 2, 9, 19, 29, and 39, all the tasks were performed in the scanner. On day 4, only the trained task and the control task were performed in the scanner. On the remaining days, the subjects performed VSWM training at home. (B) The three tasks performed in the scanner. On the top is the trained task, in the middle is the transfer task, and at the bottom is the control task.

(ICA) to remove eye movement and heartbeat artifacts, and a notch filter to remove line noise of 50 Hz and its harmonics. Both ICA and notch filtering were performed with the python toolbox MNE-Python (https://doi.org/10.5281/zenodo.592483). The preprocessing steps were done on each subject and measurement session separately.

Cortical parcellation and source reconstruction

T1-weighted structural MRI images (1 × 1 mm^2) were acquired for each subject with a 3 Tesla scanner (GE SIGNA Premier). Anatomical reconstructions from the MRIs were created using the software FreeSurfer (http://freesurfer.net/). The reconstructions were parcellated into the 200-parcel Schaefer atlas with seven networks (Schaefer et al. 2018). The signal was projected to the parcel space using minimum norm estimation (MNE) with the dSPM method using MNE-Python (Gramfort et al. 2014). Here, the noise covariance matrix was constructed for each participant and session using the 1000-ms windows between the start of the trials and the presentations of cue 1 (load 0). The dipole sources were separated by 5 mm and had a fixed orientation normal to the pial surface. To collapse the source space into parcel space we used a previously described method (Korhonen et al. 2014), which optimizes the collapse-operator by maximizing the fidelity between a simulated original time series and its reconstructed signal. However, unlike the original method, we optimized the collapse-operator numerically using the Python package PyTorch (Paszke et al. 2019).

Time frequency analysis

The parcel time-series were separated into epochs of 1600 ms spanning the delay period and 300-ms windows on either side of the delay in order to avoid edge effects during the delay periods. These windows were removed after the time frequency analysis was completed. The epochs were then sorted into loads (0–6) and trial type (trained, transfer, and control). Wavelet transformation was performed using a bank of complex Morlet wavelets with a time–frequency compromise parameter of $m = 5$ and approximately log-linearly spaced c frequencies ranging from 5 to 118 Hz. After filtering, the narrow-band data were down sampled to a sampling rate of five times the center frequency. The transformation was done using MNE-python (Cohen 2019).

Synchronization analysis

For each frequency, we calculated parcel-to-parcel synchronization using the iPLV (Palva et al. 2018) value defined as

$$iPLV = imag\left(\frac{1}{N}\sum_{n=1}^{N}\left[e^{i(\Delta\theta_n)}\right]\right)$$

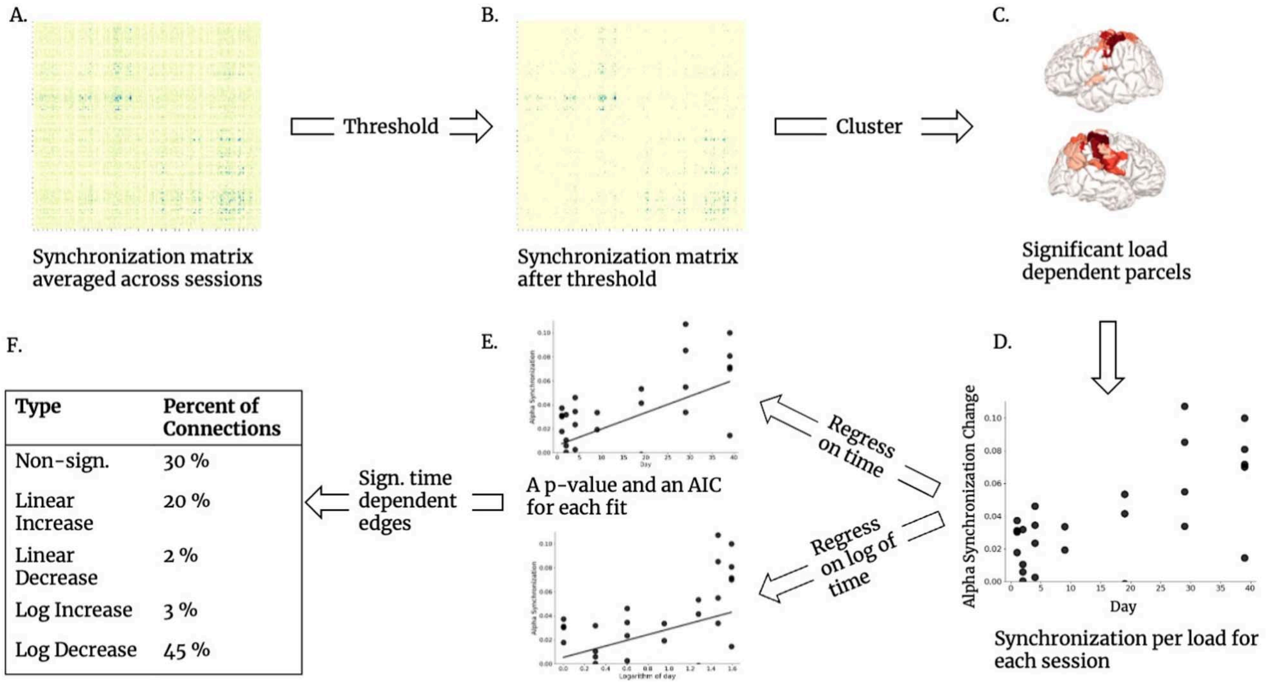

Fig. 2. The analysis pipeline. (A) The all-to-all synchronization matrix averaged across sessions and multiplied with the IEM. We had one of these for each load and participant. (B) The synchronization matrix after edges that do not have significant load-dependent increase have been set to 0. (C) The degree of edges in each brain parcel after clustering has been applied. (D) The baseline-corrected synchronizations for all loads (1–5) visualized for a random edge. (E) The regression over time, on the top regressed on days, and on the bottom regressed on the logarithm of day. (F) Example of how load-dependent edges for a subject could be divided up using the time-dependent analysis.

where $\Delta\theta$ is the phase difference between two sources and N is the number of samples in the time series. This gave us an all-to-all synchronization matrix for each trial type and load between 0 and 5. We did not calculate synchronization for load 6, as it only had half the number of trials of the other loads, meaning that its iPLV value could not be accurately compared with that of lower loads. Synchronization was computed separately for each participant and measurement session. To identify edges that could putative arise via source-leakage (Palva et al. 2018), we also created a binary intractable edge matrix (IEM) based on source-leakage (Wang et al. 2018) with 0s for intractable edges and 1s elsewhere.

Identifying load-dependent VSWM networks

Using data from the trained task only, we aimed to identify individual VSWM networks for each participant by extracting edges from the synchronization matrices where the strength increased under VSWM-load.

To identify frequencies of interest, we first computed the mean synchronization strength of all edges during measurement session one (S1). For each subject, we selected the frequency which showed the largest mean change in synchronization under load. For this load-dependent frequency, we constructed 42 synchronization matrices for each participant (one for each load and each measurement session). These matrices were then averaged across measurement sessions, resulting in six synchronization matrices per participant, one for each load (Fig. 2A). The matrices were multiplied with the IEMs to alleviate the influence of source-leakage.

From the time-averaged synchronization matrices, we extracted the specific edges where the synchronization increase with load was significant (Fig. 2B). Here, we did not want to assume a monotone increase between loads 0 and 5, since synchronization could potentially plateau or even decrease at high loads. Thus, we defined the synchronization increase of an edge as its maximum synchronization (i.e. synchronization for either load 1, 2, 3, 4, or 5) subtracted by its baseline synchronization at load 0. To define a threshold for a significant synchronization increase, we created six random synchronization matrices, representing loads 0–5, by shuffling the synchronization matrix for load 0 six times. We then calculated the synchronization increases for the edges of these shuffled matrices. This procedure was repeated 1000 times giving us a probability distribution of random synchronization increase. The top 99th quantile was defined as the threshold for a significant synchronization increase.

To remove remaining spurious findings arising from multiple comparisons, we performed a cluster analysis. Here, we discarded edges connected to parcels with less than five other connections, yielding 97.5% of the spurious connections. These remaining edges were used to define a load-dependent synchronization network for each subject (Fig. 2C).

All analysis was performed on an individual subject level. To later investigate consistencies in VSWM networks between individuals, we calculated Pearson correlations between the averaged synchronization matrices (Fig. 2A).

Identifying time-dependent changes in synchronization

After a load-dependent VSWM network was defined for each participant, we next investigated the changes within the network over training sessions. Here again, all analysis was performed for the trained task only.

First, the synchronization at load 0 was subtracted from loads 1 to 5, to correct for baseline synchronization. The synchronizations for load 1 to 5 were then regressed over training session (Fig. 2D). To differentiate between fast changes that occur within the first sessions and could reflect strategy development, from slow linear changes that possibly reflect capacity improvement, we used both linear and log-based regression (Fig. 2E). Edges with significant regression coefficients ($P < 0.05$) were extracted and multiple comparison corrected using false discovery rate (FDR). If a synchronization change was significant using both linear and log-based regression, we chose the regression with the best fit calculated using Akaike Information Criterion (AIC). Thus, all edges were separated into five groups—linear increase, linear decrease, logarithmic increase, logarithmic decrease, and no significant change (Fig. 2F).

Testing transfer effect

Finally, when time-dependent changes in the trained task had been identified within the load-dependent VSWM networks, we tested if these changes were transferable. A transferable change was defined as a change that occurred both in the transfer task and in the trained task, but not in the control task. To quantify changes over training session in the control and transfer tasks, we used the synchronization between loads 1 and 5 rather than the difference between loads 1 and 5 and baseline (load 0). This was because we did not expect any load dependency in the control task and thus, subtracting by the baseline at each session could potentially remove any time-dependent changes. To make the comparison fair, we did not subtract by baseline in the transfer task either.

Results

Behavioral results

According to our model, all four subjects had an initial task specific improvement in the first 2–5 days as well as a linear capacity improvement during the VSWM training program (Fig. 3). The capacity (β_{cap}) increased significantly in all four subjects (β_{cap}= 0.029, 0.025, 0.032, and 0.048 levels per training day, $P < 0.05$, one-tailed), consistent with prior reports (Ericson and Klingberg 2023).

MEG results

Identifying a load-dependent VSWM network

We first visualized the mean synchronization strength for each load in the trained task as a function of frequency (Fig. 4A–D). In all participants, the mean synchronization had a peak in the alpha-frequency band. However, the function of load dependency differed between participants. While two participants had a load-dependent increase throughout the trial (Fig. 4B, D), the alpha synchronization returned to baseline at the end of the trial for the other two participants (Fig. 4A, C). Furthermore, the frequency of the individual alpha peaks differed. Two participants had an alpha peak at 11 Hz (Fig. 4B, C), while the other two had an alpha peak at 10 Hz (Fig. 4A, D). We also visualized a rolling average of alpha synchronization throughout the trial. Alpha synchronization increased during the delay period but decreased during encoding, ramping up as a function load (Fig. 4E).

For the individual alpha peaks, we next identified load-dependent VSWM networks using only data from the trained task. The VSWM networks consisted of edges with a significant alpha synchronization increase. These networks varied between individuals (Fig. 5A–D), especially for one subject where the network had much more activation in temporal areas compared to others (Fig. 5D). However, there was no significant correlation between the networks of any subjects ($P > 0.05$). Even though there were large inter-individual differences, the differences within individuals over time were smaller (Fig. 5E). If one network was extracted per session and individual, the within participant networks all correlated significantly ($P < 0.05$).

Identifying training related changes within the VSWM network

Within the identified VSWM networks, we extracted edges where there was a linear strengthening of synchronization over training session, as this could reflect capacity improvements (Fig. 2E). Three participants showed such a time-dependent increase in the alpha band within parietal, somatomotor, and frontal regions (Fig. 6A–C, FDR corrected with $P < 0.05$). When investigating similarities in the synchronization increase between the three subjects, we found an overlap around the intraparietal and superior parietal cortex, and in the superior frontal gyrus around the frontal eye field (Fig. 6D).

Testing the training related changes for transfer

To verify that the synchronization increase observed in the trained task was transferable, we analyzed if the edges (Fig. 6A–C) were also strengthened in the transfer task without being strengthened in the control task. In all three participants, there was a significant increase of synchronization in the transfer task ($P = 0.004$, 0.000, and 0.000) but not in the control task ($P = 0.188$, 0.064, 0.178) (Fig. 7), thus verifying that the linear synchronization increase observed in the trained task was transferable.

Behavioral and neural changes in subject 3

Subject 3 did not show an increase of alpha synchronization over time. After closer inspection we found that there was a switch in synchronization frequency from alpha to theta starting in S3 (Fig. 8A–F). The theta network had a very different architecture compared to the alpha network (Fig. 8G). We did not find transferable time-dependent changes in this theta network.

When investigating the behavioral result, we found that the model fit for subject 3 was the worst. This was related to the fact that subject 3 had a performance drop below the baseline level on the fourth day (Fig. 8H). If we removed the first 3 days from subject 3's behavioral data and start the analysis on day 4, which had the lowest performance overall, the pattern changed. Now we again saw a quick increase to begin, but the capacity component ($\beta_{cap} = 0.001$) was not significantly positive (Fig. 8I).

The observed alterations in both network structure and frequency during the first week of training suggest a strategy change. This is also supported by the fact that the switch happened abruptly, that the theta increase did not transfer to the transfer task, and because no behavioral capacity improvement occurred when the behavioral data was reanalyzed using day 4 as a baseline.

Discussion

Here we aimed to identify neural mechanisms underlying transfer after VSWM training. To be congruent with the linear increase of the capacity component in our prior behavioral study (Ericson and Klingberg 2023), we hypothesized that VSWM transfer would correspond to a linear strengthening of synchronization within individual networks that also show a load-dependency.

First, we analyzed behavioral improvement in the training program. We used the previously developed HMM algorithm to divide the improvement up into a task-specific strategy component and a capacity component (Ericson and Klingberg 2023). According to

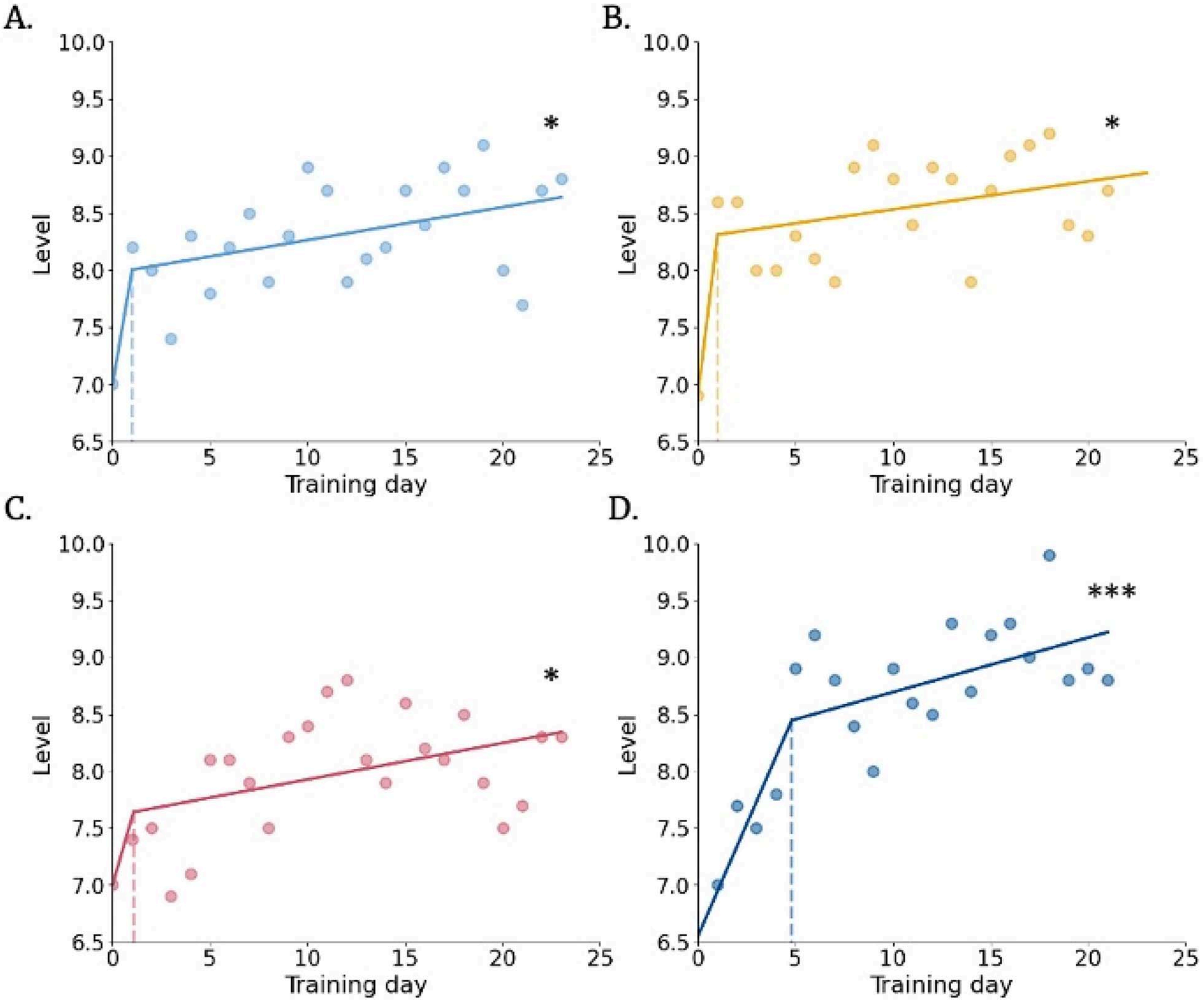

Fig. 3. The behavioral changes from VSWM training analyzed using the HMM (Ericson and Klingberg 2023). (A) Subjects 1, (B) Subject 2, (C) Subject 3, and (D) Subject 4. $^*P < 0.05$, $^{***}P < 0.001$.

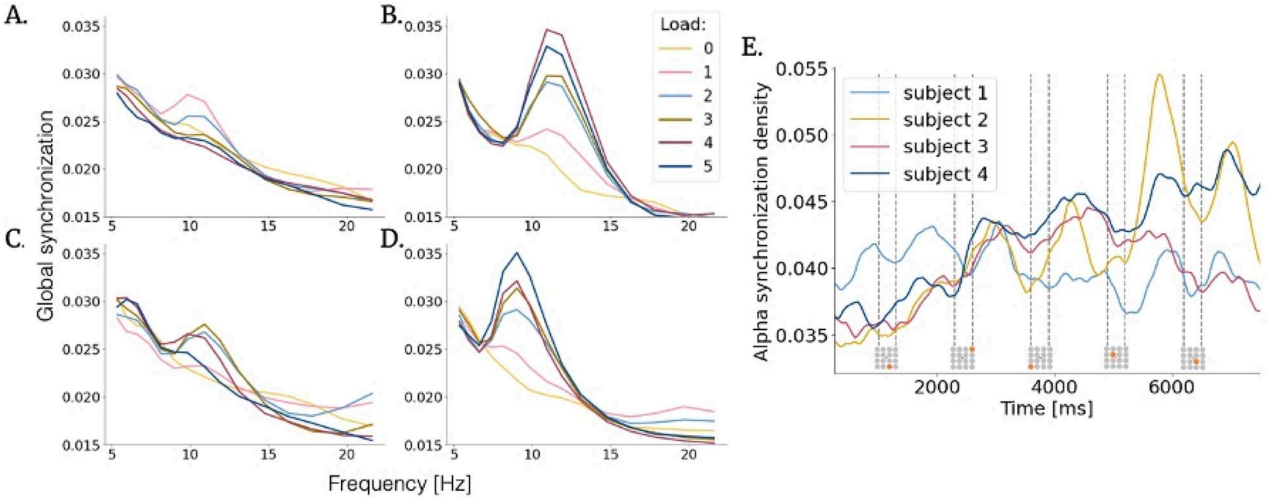

Fig. 4. Global synchronization pattern from S1. (A)–(D) Synchronization density for the delay periods of each load for subjects 1–4, respectively. (E) A rolling average of synchronization at the alpha peak for the whole trial. The dotted lines mark the beginning and end of cue presentations.

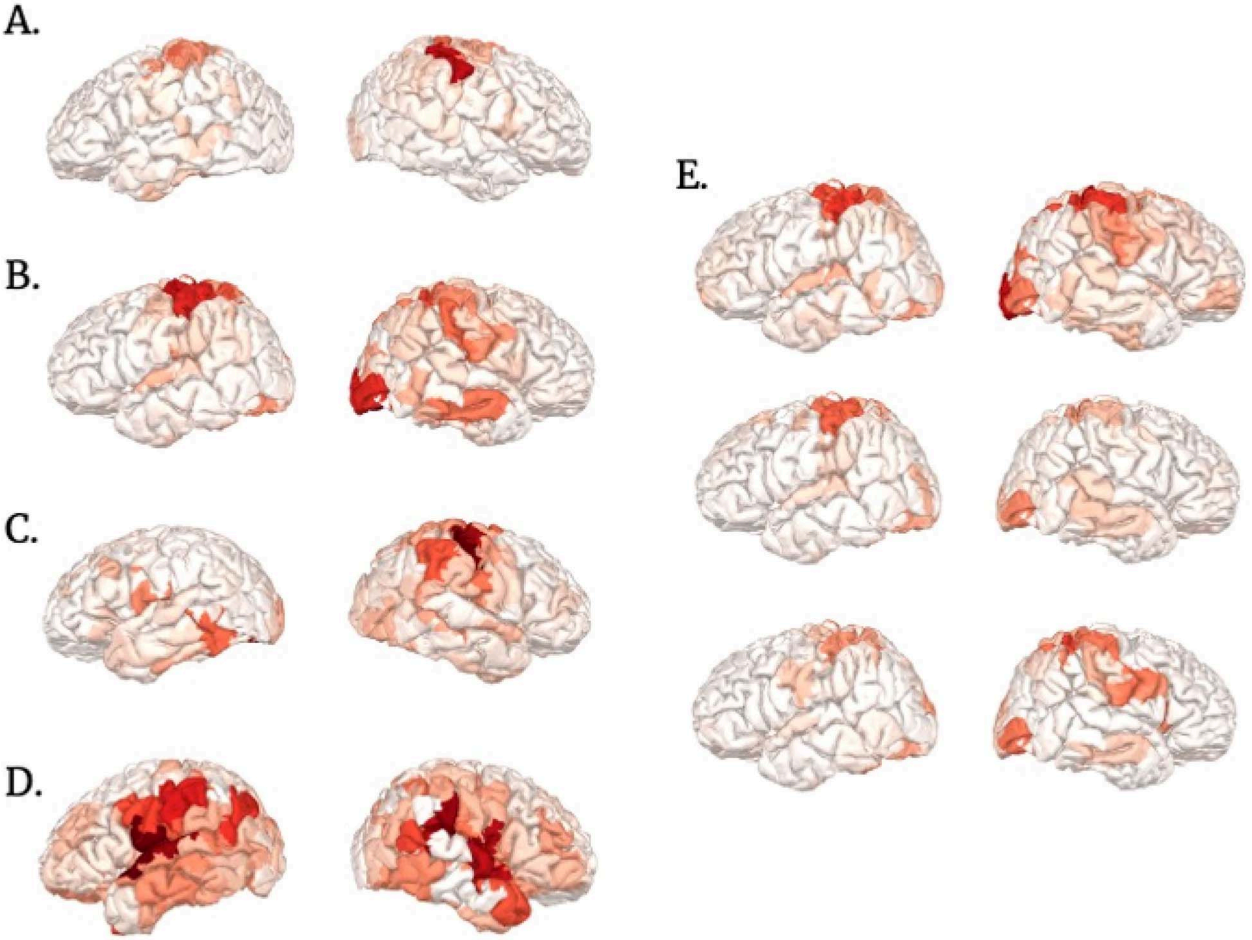

Fig. 5. The degree of synchronization for each parcel in the load-dependent network. (A)–(D) The degree for subjects 1–4, respectively, calculated using the time-averaged synchronization matrices. (E) The degree for subject 2 from S1, S2, and S7.

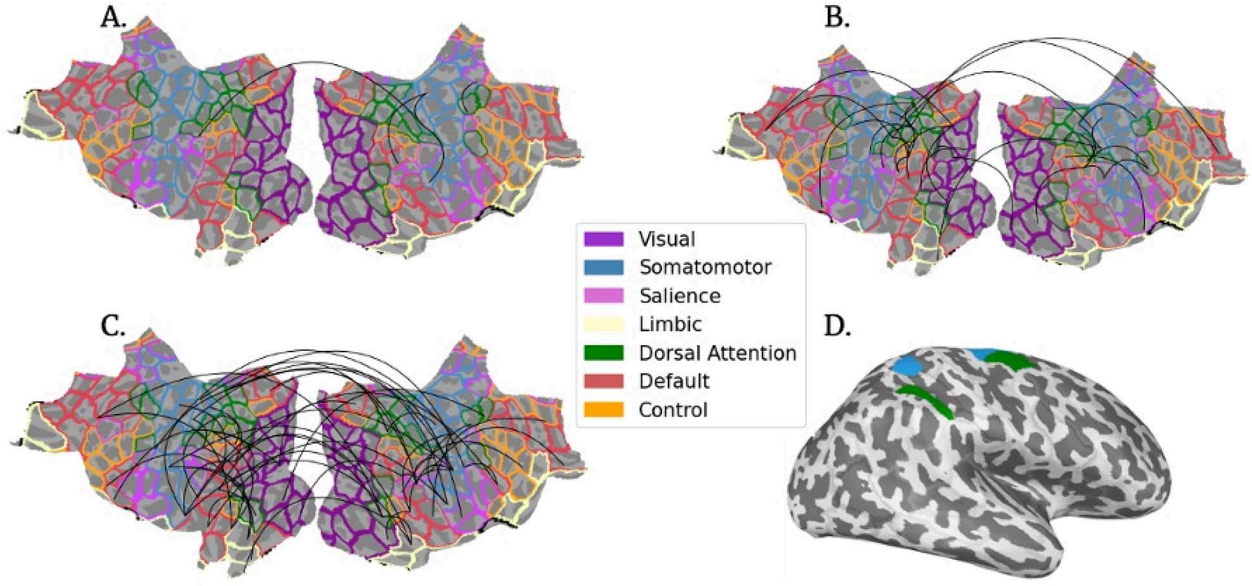

Fig. 6. Results from the regressions. (A)–(C) Flat maps showing edges with significant time-dependent linear increase of alpha synchronization. (A) Subject 1, (B) Subject 2, and (C) Subject 4. (D) Parcels that overlap in all three subjects. The overlapping parcels are color coded to their corresponding networks.

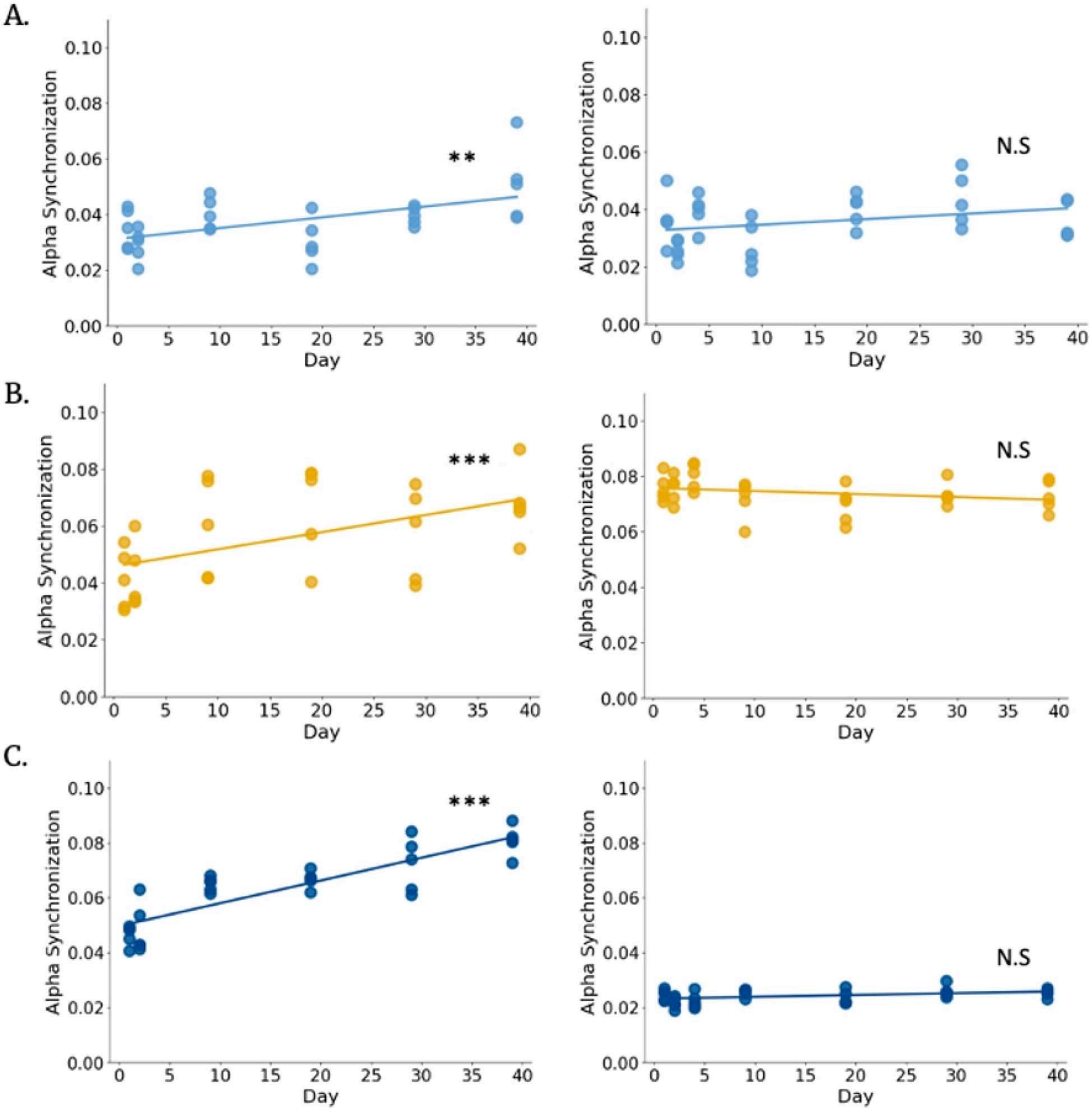

Fig. 7. Changes in synchronization for the edges that show a linear strengthening of synchronization in the trained task. To the left is the change in the transfer task and to the right is the change in the control task. $^{**}P < 0.005$, $^{***}P < 0.001$. (A) Subjects 1, (B) Subject 2, and (C) Subject 4.

the model, all participants had a positive capacity component, showing an increase of capacity during training. The change from the first phase, with both strategy and capacity, to the second phase of only capacity occurred between training days 2 and 5 (Fig. 3).

Next, we defined an individual load-dependent VSWM network for each participant using MEG data from a trained task. Within these networks, we investigated if there was a linear strengthening of synchronization over training sessions for the trained task. We found an increase of alpha synchronization in three out of four participants. This pattern was most consistent across the intraparietal and superior parietal cortices, and in the superior frontal gyrus around the frontal eye field. The activity of these specific brain regions are known to correlate with VSWM (Rottschy et al. 2012). The same increase was also observed in the transfer task, but not in the control task. The transfer effect suggests that a strengthening of alpha synchronization is related to a VSWM capacity increase and not to a task specific improvement.

The within-participant design revealed consistency in both network architecture and peak frequency across time. Notably, it was possible to define the VSWM networks by identifying significant load-dependent changes within single subjects, and therefore without restricting the analysis to predefined regions of interest. Similarly, training-induced changes also exhibited significance at the individual level, effectively making each subject a self-contained replication of the findings.

Alpha synchronization has previously been linked with VSWM capacity (Sauseng et al. 2009; Palva et al. 2010; Riddle et al. 2020), but it has also been associated with visuospatial attention (Lobier et al. 2018; D'Andrea et al. 2019). This aligns with the notion

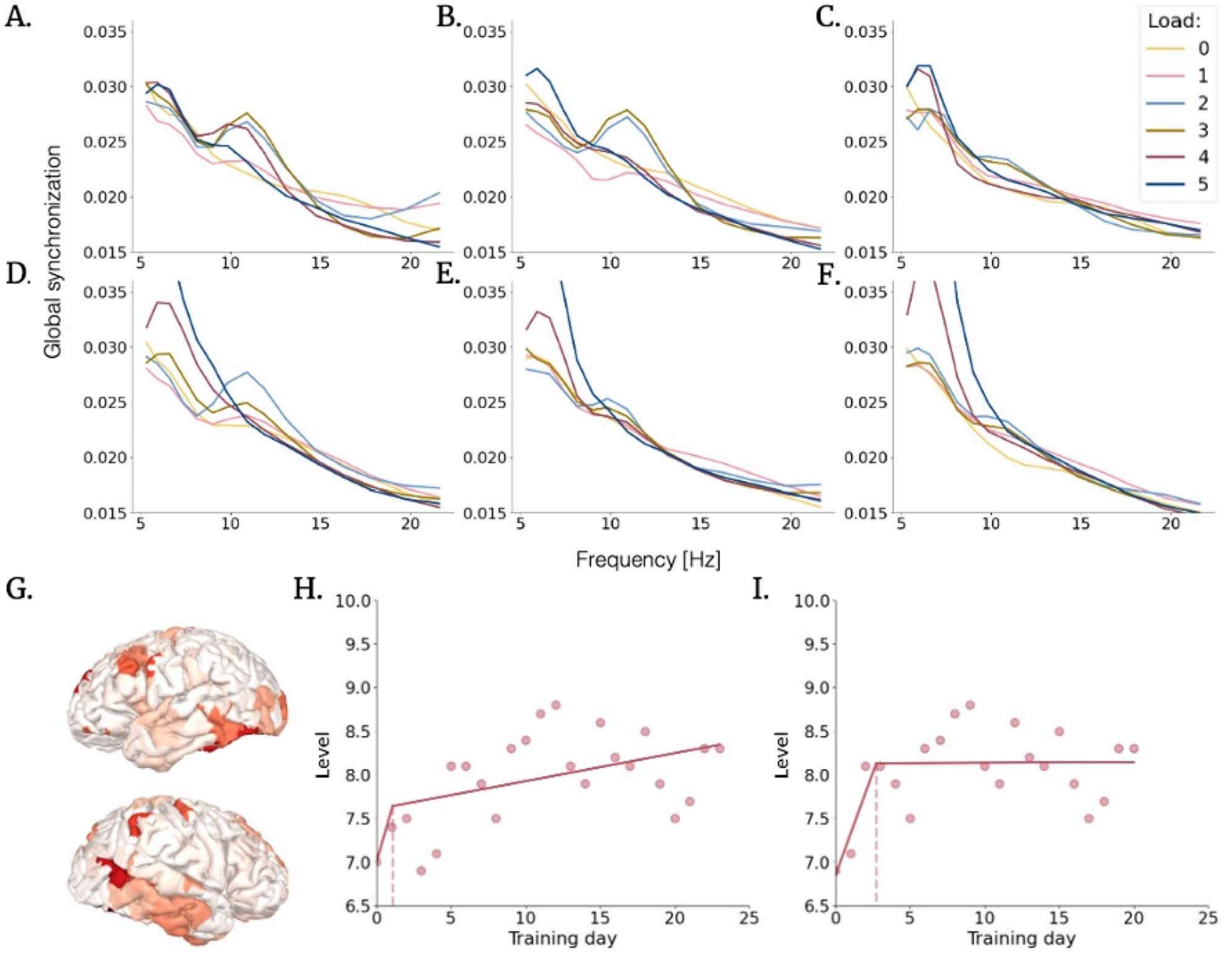

Fig. 8. An analysis of subject 3 related to the change of alpha to theta synchronization. (A) – (F) The synchronization density for S2–S7. (G) The synchronization degree for the theta network. (H) The original HMM of the behavioral data. (I) The HMM without the first 3 days.

that the control of visuospatial attention and VSWM share a common neural substrate (Ikkai and Curtis 2011; Panichello and Buschman 2021). As such, the strengthening of alpha synchronization could also translate into improvements in visuospatial attention, explaining why VSWM training can yield enhancements in non-VSWM cognitive tasks (Klingberg et al. 2005; Jaeggi et al. 2008; Schmiedek et al. 2010).

The specific role of alpha synchronization in VSWM and visuospatial attention remains a subject of speculation. Nevertheless, a clue might be found in studies of visual processing (Kastner et al. 2020). In both humans and monkeys, the processing of new visual information is dynamic, alternating between periods of high and low processing. For example, low visual processing occurs during eye saccades and may serve as a crucial mechanism for maintaining visual stability during rapid eye movements. Intriguingly, intracranial recordings from monkeys show that periods of low visual processing are characterized by a parietal-driven alpha synchronization. A similar mechanism might be adapted in VSWM tasks, where attention should also focus on internally maintained items during delays rather than external stimuli. However, more translational research is needed in order to link intracranial findings in primates with similar electrophysiology mechanisms in humans.

In terms of structural changes, enhanced synchronization has been linked to both white matter and synaptic plasticity (Womelsdorf et al. 2007; Uhlhaas et al. 2010). Both these processes operate over a period of weeks (Buonomano and Merzenich 1998; Bonetto et al. 2021), matching the temporal dynamics of capacity improvement. While a gradual increase of cortical activation in prefrontal regions has been observed in electrophysiological recordings in monkeys after VSWM training (Qi et al. 2011), white matter plasticity in the frontoparietal network is documented both in development (Klingberg 2006; Peters et al. 2012) and training (Takeuchi et al. 2010; Caeyenberghs et al. 2016), and is likely related to an increased myelination in the superior longitudinal fasciculus (Metzler-Baddeley et al. 2017). Thus, both processes are probable candidates for the structural alterations responsible for the enhanced synchronization.

Finally, it is important to note that the alpha synchronized network could also encompass subcortical regions, which are difficult to measure with MEG. For example, certain parts of the striatum contain fibers originating from both prefrontal and parietal regions (Selemon and Goldman-Rakic 1988; Haber 2003; Darki and Klingberg 2018). Maturation of these convergent striatal regions has been correlated with frontoparietal connectivity and executive functions, including VSWM capacity, during childhood (Darki et al. 2020). Furthermore, synchronicity in particularly in the alpha-frequency has often been associated with thalamocortical interconnections (Hughes and Crunelli 2005).

Even though the VSWM networks were consistent within subjects, there were large interindividual differences between the subjects. One of the most pronounced individual patterns was the switch from alpha to theta activity in one subject. A large-N, group-study of training, might have found an average increase of both alpha and theta during the training period. However, the within-participant analysis revealed that the increase of theta in subject 3 actually coincided with a reduction of alpha synchronization. This highlights a major benefit of within-participant designs.

A drawback with a small N-design is that it will always be limited by the fact that interindividual analyses are underpowered. We could for example not compare the behavioral improvement to the change of synchronization between subjects. A larger sample size is needed in order to answer such questions.

We did not find any consistent neural changes related to early, task specific improvements, even though the largest behavioral improvements occurred in the beginning of the training period (Fig. 3). There were neural changes within single subjects during the first three measurements, the most obvious being the switch from alpha to theta activity in subject 3, but these effects could not be replicated in other subjects. One possibility is that task-specific changes are in fact very individual, and thereby difficult to replicate. It is also possible that implicit strategies, such as automatization of stimulus response rules, develop during encoding rather than the maintenance period which was analyzed in the present study.

In conclusion, in three out of four participants, VSWM training led to an increased alpha synchronization in a network with interindividual overlap around the intraparietal sulcus and the frontal eye field. An increase of alpha synchronization within the same network was also identified in the transfer task but not in the control task. This suggests that increased frontoparietal alpha synchronization could be a neural correlate of transfer in VSWM training.

Acknowledgments

We would like to thank Jeanie Dawnbringer who helped to collect MEG data and write visualization scripts for the brain images.

CRediT author statement

Julia Ericson (Conceptualization, Data curation, Formal analysis, Investigation, Methodology, Project administration, Visualization, Writing—original draft), Satu Palva (Conceptualization, Methodology, Writing—review and editing), J. Matias Palva (Conceptualization, Methodology), Torkel Klingberg (Conceptualization, Formal analysis, Funding acquisition, Investigation, Methodology, Project administration, Supervision, Visualization, Writing—original draft).

Funding

This work was supported by Marianne and Marcus Wallenbergs Stiftelse (MMW 2020.0064).

Conflict of interest statement: None declared.

References

Astle DE, Barnes JJ, Baker K, Colclough GL, Woolrich MW. Cognitive training enhances intrinsic brain connectivity in childhood. *J Neurosci*. 2015:35(16):6277–6283.

Berger B, Griesmayr B, Minarik T, Biel AL, Pinal D, Sterr A, Sauseng P. Dynamic regulation of interregional cortical communication by slow brain oscillations during working memory. *Nat Commun*. 2019:10(1):4242.

Bergman-Nutley S, Klingberg T. Effect of working memory training on working memory, arithmetic and following instructions. *Psychol Res*. 2014:78(6):869–877.

Bonetto G, Belin D, Káradóttir RT. Myelin: A gatekeeper of activity-dependent circuit plasticity? *Science*. 2021:374(6569):374, eaba6905.

Buonomano DV, Merzenich MM. Cortical plasticity: from synapses to maps. *Annu Rev Neurosci*. 1998:21(1):149–186.

Caeyenberghs K, Metzler-Baddeley C, Foley S, Jones DK. Dynamics of the human structural connectome underlying working memory training. *J Neurosci*. 2016:36(14):4056–4066.

Chen X, Ma R, Zhang W, Zeng GQ, Wu Q, Yimiti A, Xia X, Cui J, Liu Q, Meng X. Alpha oscillatory activity is causally linked to working memory retention. *PLoS Biol*. 2023:21(2):e3001999.

Cohen MX. A better way to define and describe Morlet wavelets for time-frequency analysis. *NeuroImage*. 2019:199:81–86.

Constantinidis C, Klingberg T. The neuroscience of working memory capacity and training. *Nat Rev Neurosci*. 2016:17(7):438–449.

D’Andrea A, Chella F, Marshall TR, Pizzella V, Romani GL, Jensen O, Marzetti L. Alpha and alpha-beta phase synchronization mediate the recruitment of the visuospatial attention network through the superior longitudinal fasciculus. *NeuroImage*. 2019:188:722–732.

Darki F, Klingberg T. Functional differentiation between convergence and non-convergence zones of the striatum in children. *NeuroImage*. 2018:173:384–393.

Darki F, Sauce B, Klingberg T. Inter-individual differences in striatal connectivity is related to executive function through fronto-parietal connectivity. *Cereb Cortex*. 2020:30(2):672–681.

Ericson J, Klingberg T. A dual-process model for cognitive training. *NPJ Sci Learn*. 2023:8(1):12.

Ericsson KA, Chase WG, Faloon S. Acquisition of a memory skill. *Science*. 1980:208(4448):1181–1182.

Fisher AJ, Medaglia DJ, Jeronimus BF. Lack of group-to-individual generalizability is a threat to human subjects research. *Proc Natl Acad Sci U S A*. 2018:115(27):E6106–E6115.

Gathercole SE, Durling E, Evans M, Jeffcock S, Stone S. Working memory abilities and children’s performance in laboratory analogues of classroom activities. *Appl Cogn Psychol*. 2008:22(8): 1019–1037.

Gathercole SE, Dunning DL, Holmes J, Norris D. Working memory training involves learning new skills. *J Mem Lang*. 2019:105: 19–42.

Gramfort A, Luessi M, Larson E, Engemann DA, Strohmeier D, Brodbeck C, Parkkonen L, Hämäläinen MS. MNE software for processing MEG and EEG data. *NeuroImage*. 2014:86:446–460.

Haber SN. The primate basal ganglia: parallel and integrative networks. *J Chem Neuroanat*. 2003:26(4):317–330.

Hughes SW, Crunelli V. Thalamic mechanisms of EEG alpha rhythms and their pathological implications. *Neuroscientist*. 2005:11(4): 357–372.

Ikkai A, Curtis CE. Common neural mechanisms supporting spatial working memory, attention and motor intention. *Neuropsychologia*. 2011:49(6):1428–1434.

Ince RA, Kay JW, Schyns PG. Within-participant statistics for cognitive science. *Trends Cogn Sci*. 2022:8(8):620–630.

Jaeggi SM, Buschkuehl M, Jonides J, Perrig WJ. Improving fluid intelligence with training on working memory. *Proc Natl Acad Sci U S A*. 2008:105(19):6829–6833.

Jolles DD, van Buchem MA, Crone EA, Rombouts SA. Functional brain connectivity at rest changes after working memory training. *Hum Brain Mapp*. 2013:34(2):396–406.

Judd N, Klingberg T. Training spatial cognition enhances mathematical learning in a randomized study of 17,000 children. *Nat Hum Behav*. 2021:5(11):1548–1554.

Kastner S, Fiebelkorn IC, Eradath MK. Dynamic pulvino-cortical interactions in the primate attention network. *Curr Opin Neurobiol*. 2020:65:10–19.

Katz B, Shah P, Meyer DE. How to play 20 questions with nature and lose: reflections on 100 years of brain-training research. *Proc Natl Acad Sci U S A*. 2018:115(40):9897–9904.

Klingberg T. Development of a superior frontal–intraparietal network for visuo-spatial working memory. *Neuropsychologia*. 2006:44(11):2171–2177.

Klingberg T, Fernell E, Olesen PJ, Johnson M, Gustafsson P, Dahlström K, Gillberg CG, Forssberg H, Westerberg H. Computerized training of working memory in children with ADHD-a randomized, controlled trial. *J Am Acad Child Adolesc Psychiatry*. 2005:44(2):177–186.

Korhonen O, Palva S, Palva JM. Sparse weightings for collapsing inverse solutions to cortical parcellations optimize M/EEG source reconstruction accuracy. *J Neurosci Methods*. 2014:226:147–160.

Kundu B, Sutterer DW, Emrich SM, Postle BR. Strengthened effective connectivity underlies transfer of working memory training to tests of short-term memory and attention. *J Neurosci*. 2013:33(20): 8705–8715.

Lobier M, Palva JM, Palva S. High-alpha band synchronization across frontal, parietal and visual cortex mediates behavioral and neuronal effects of visuospatial attention. *NeuroImage*. 2018:165: 222–237.

Metzler-Baddeley C, Foley S, de Santis S, Charron C, Hampshire A, Caeyenberghs K, Jones DK. Dynamics of white matter plasticity underlying working memory training: multimodal evidence from diffusion MRI and relaxometry. *J Cogn Neurosci*. 2017:29(9): 1509–1520.

Molenaar PC. A manifesto on psychology as idiographic science: bringing the person back into scientific psychology, this time forever. *Measurement*. 2004:2(4):201–218.

Palva JM, Monto S, Kulashekhar S, Palva S. Neuronal synchrony reveals working memory networks and predicts individual memory capacity. *Proc Natl Acad Sci U S A*. 2010:107(16):7580–7585.

Palva S, Kulashekhar S, Hämäläinen M, Palva JM. Localization of cortical phase and amplitude dynamics during visual working memory encoding and retention. *J Neurosci*. 2011:31(13): 5013–5025.

Palva JM, Wang SH, Palva S, Zhigalov A, Monto S, Brookes MJ, Schoffelen JM, Jerbi K. Ghost interactions in MEG/EEG source space: a note of caution on inter-areal coupling measures. *NeuroImage*. 2018:173:632–643.

Panichello MF, Buschman TJ. Shared mechanisms underlie the control of working memory and attention. *Nature*. 2021:592(7855): 601–605.

Paszke A, Gross S, Massa F, Lerer A, Bradbury J, Chanan G, Killeen T, Lin Z, Gimelshein N, Antiga L. Pytorch: an imperative style, high-performance deep learning library. *Adv Neural Inf Process Syst*. 2019:32:8024–8035.

Peters BD, Szeszko PR, Radua J, Ikuta T, Gruner P, DeRosse P, Zhang JP, Giorgio A, Qiu D, Tapert SF. White matter development in adolescence: diffusion tensor imaging and meta-analytic results. *Schizophr Bull*. 2012:38(6):1308–1317.

Qi XL, Meyer T, Stanford TR, Constantinidis C. Changes in prefrontal neuronal activity after learning to perform a spatial working memory task. *Cereb Cortex*. 2011:21(12):2722–2732.

Riddle J, Scimeca JM, Cellier D, Dhanani S, D'Esposito M. Causal evidence for a role of theta and alpha oscillations in the control of working memory. *Curr Biol*. 2020:30(9):1748–1754.e4.

Rottschy C, Langner R, Dogan I, Reetz K, Laird AR, Schulz JB, Fox PT, Eickhoff SB. Modelling neural correlates of working memory: a coordinate-based meta-analysis. *NeuroImage*. 2012:60(1):830–846.

Roux F, Uhlhaas PJ. Working memory and neural oscillations: alpha–gamma versus theta–gamma codes for distinct WM information? *Trends Cogn Sci*. 2014:18(1):16–25.

Sauseng P, Klimesch W, Heise KF, Gruber WR, Holz E, Karim AA, Glennon M, Gerloff C, Birbaumer N, Hummel FC. Brain oscillatory substrates of visual short-term memory capacity. *Curr Biol*. 2009:19(21):1846–1852.

Sauseng P, Peylo C, Biel AL, Friedrich EV, Romberg-Taylor C. Does cross-frequency phase coupling of oscillatory brain activity contribute to a better understanding of visual working memory? *Br J Psychol*. 2019:110(2):245–255.

Schaefer A, Kong R, Gordon EM, Laumann TO, Zuo XN, Holmes AJ, Eickhoff SB, Yeo BT. Local-global parcellation of the human cerebral cortex from intrinsic functional connectivity MRI. *Cereb Cortex*. 2018:28(9):3095–3114.

Schmiedek F, Lövdén M, Lindenberger U. Hundred days of cognitive training enhance broad cognitive abilities in adulthood: findings from the COGITO study. *Front Aging Neurosci*. 2010:2:27.

Selemon LD, Goldman-Rakic PS. Common cortical and subcortical targets of the dorsolateral prefrontal and posterior parietal cortices in the rhesus monkey: evidence for a distributed neural network subserving spatially guided behavior. *J Neurosci*. 1988:8(11): 4049–4068.

Shiffrin RM, Schneider W. Controlled and automatic human information processing: II. Perceptual learning, automatic attending and a general theory. *Psychol Rev*. 1977:84(2):127–190.

Siebenhühner F, Wang SH, Palva JM, Palva S. Cross-frequency synchronization connects networks of fast and slow oscillations during visual working memory maintenance. *Elife*. 2016:5:1–31, e13451.

Smid CR, Karbach J, Steinbeis N. Toward a science of effective cognitive training. *Curr Dir Psychol*. 2020:29(6):531–537.

Smith PL, Little DR. Small is beautiful: in defense of the small-N design. *Psychon Bull Rev*. 2018:25(6):2083–2101.

Takeuchi H, Sekiguchi A, Taki Y, Yokoyama S, Yomogida Y, Komuro N, Yamanouchi T, Suzuki S, Kawashima R. Training of working memory impacts structural connectivity. *J Neurosci*. 2010:30(9): 3297–3303.

Thiebaut de Schotten M, Forkel SJ. The emergent properties of the connected brain. *Science*. 2022:378(6619):505–510.

Uhlhaas PJ, Roux F, Rodriguez E, Rotarska-Jagiela A, Singer W. Neural synchrony and the development of cortical networks. *Trends Cogn Sci*. 2010:14(2):72–80.

Wang SH, Lobier M, Siebenhühner F, Puoliväli T, Palva S, Palva JM. Hyperedge bundling: A practical solution to spurious interactions in MEG/EEG source connectivity analyses. *NeuroImage*. 2018:173: 12–622.

Womelsdorf T, Schoffelen JM, Oostenveld R, Singer W, Desimone R, A. Engel AK, Fries P. Modulation of neuronal interactions through neuronal synchronization. *Science*. 2007:316(5831): 1609–1612.